UNIVERSITY OF CALIFORNIA, SAN DIEGO
SCRIPPS INSTITUTION OF OCEANOGRAPHY
VISIBILITY LABORATORY
SAN DIEGO, CALIFORNIA 92152

ATMOSPHERIC OPTICAL MEASUREMENTS IN THE VICINITY OF CRATER LAKE, OREGON. PART II.

Almerian R. Boileau

SIO Ref. 68-19

July 1968

AFCRL, U. S. Air Force, Bedford, Massachusetts
Air Force Tasks P-7621 and P66220
Naval Ship Systems Command, Washington, D. C.
Contract NObsr-95251, Task II
Project Serial No. SF0180201, Task 538

Approved:

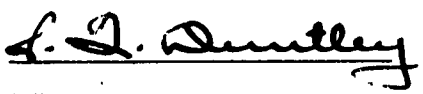

Seibert Q. Duntley, Director
Visibility Laboratory

Approved for Distribution:

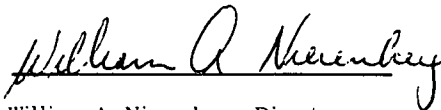

William A. Nierenberg, Director
Scripps Institution of Oceanography

ERRATA – SEPTEMBER 1968

The following corrections apply to SIO Ref. 68-18, **ATMOSPHERIC OPTICAL MEASUREMENTS in the Vicinity of Crater Lake, Oregon, Part I**, and SIO Ref. 68-19, **ATMOSPHERIC OPTICAL MEASUREMENTS in the Vicinity of Crater Lake, Oregon, Part II.**

SIO Ref. 68-18, Part I

Page	Location	Reads	Should Read
17	Figure 14 (Replace reflectance scale magnitude values)	0.001 0.010	0.010 0.100
18	Figure 15 – Replace entire page		

SIO Ref. 68-19, Part II

1	Abstract, lines 2 and 3, second sentence	Three of the descents were before local apparent noon, the fourth descent was after local apparent noon.	All descents were before local apparent noon. Simultaneous . . .
2	The Flight, last sentence, paragraph 2	Local apparent noon occurred between the third and fourth descents, at approximately 1215.	Local apparent noon occurred at approximately 1315.
6	Figure 3 Caption, lines 3, 4, and 5	Delete the last sentence on this Figure Caption.	
9	Figure 6 (Replace horizontal path function scale magnitude values in both graphs)	150 150	500 500
20	Figure 17 (Replace reflectance scale magnitude values in both graphs)	0.001 0.010 0.001 0.010	0.010 0.100 0.010 0.100
23	Figure 20 (Replace entire page)		
24	Figure 21 (Replace entire page)		
	DD Form 1473, Abstract, lines 2 and 3 second sentence	Three of the descents were before local apparent noon; the fourth descent was after local apparent noon.	All descents were before local apparent noon. Simultaneous . . .

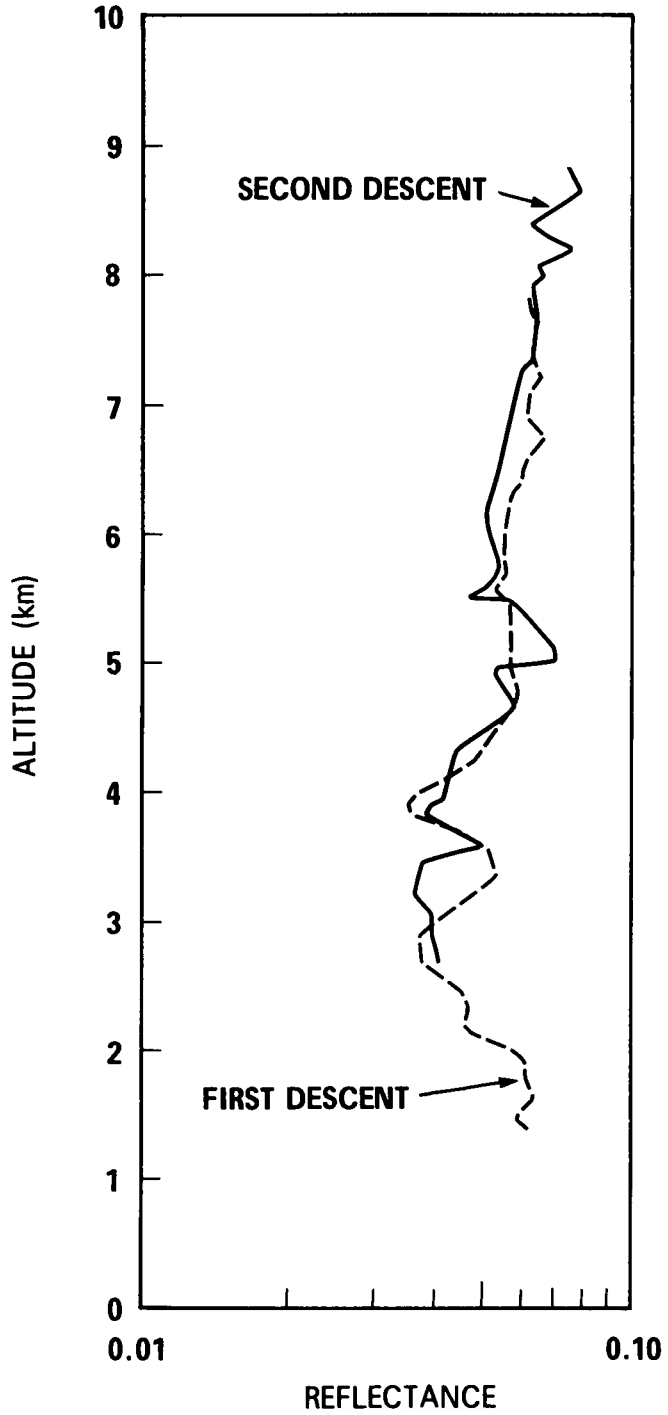

Fig. 14. Ratios of upwelling and downwelling illuminances during both descents.

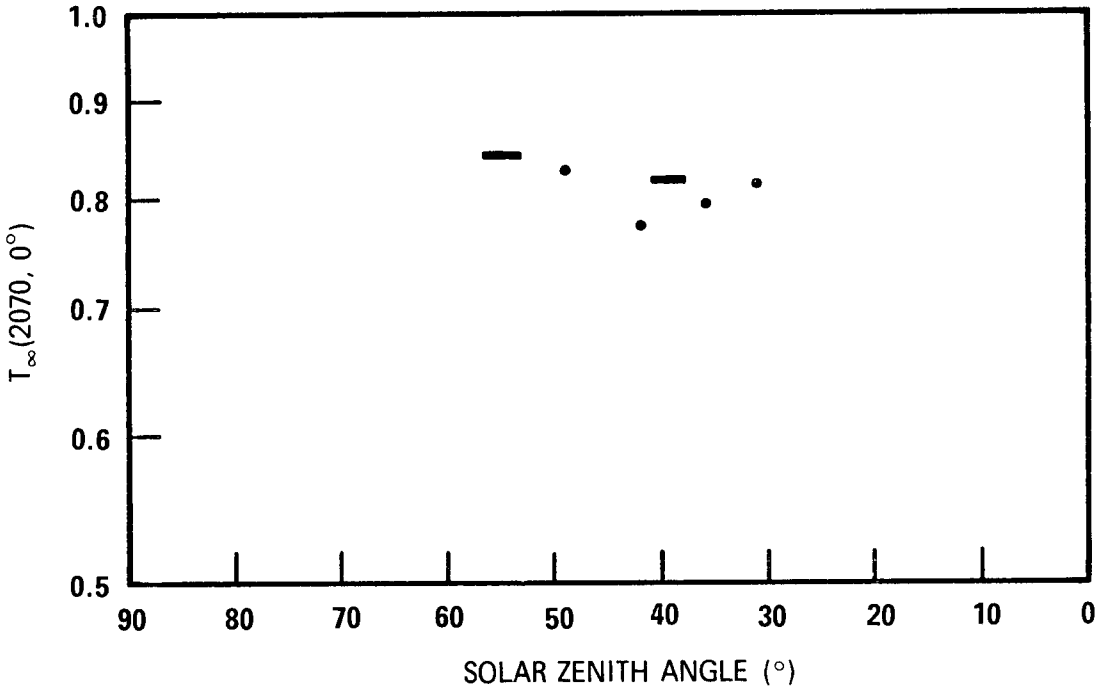

Fig. 15. Beam transmittances for vertical path of sight as a function of solar zenith angle. The four data points represent transmittances calculated from the ground-based transmissometer. The two elongated data points represent the transmittances calculated from aircraft data, extrapolated to ground level, the amount of elongation representing the change of solar zenith angle during the time of each descent.

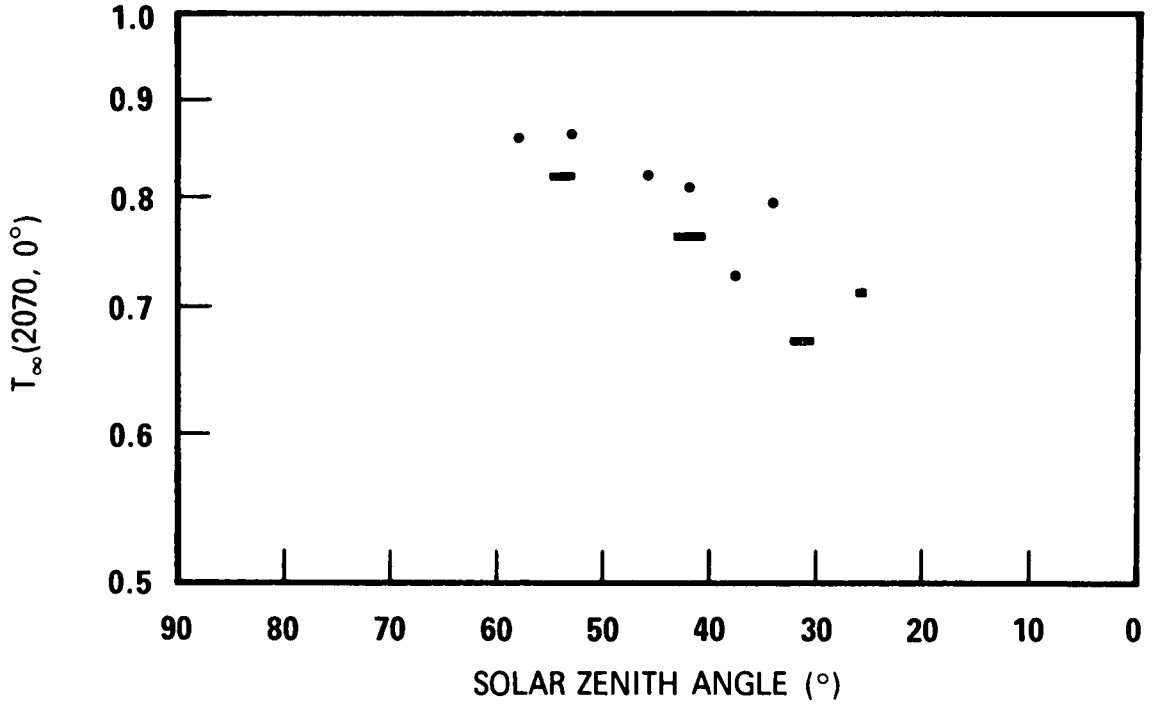

Fig. 20. Beam transmittance for the vertical path of sight as a function of the solar zenith angle. The data shown by filled circles were calculated from ground-based data and the equation

$$T_\infty(2070, 0°, 0°) = \left[\frac{{}_sB_\infty(2070, \theta_s, \phi_s)}{{}_sB_o}\right]^{\cos \theta_s}$$

The data shown by elongated data points were from extrapolated aircraft data and the equation

$$T_\infty(2070, 0°, 0°) = \exp\left[-\Sigma \Delta z / L(z)\right].$$

During the forenoon the beam transmittance for the vertical path of sight decreased as the solar zenith angle decreased. At 1315 (local apparent noon) the solar zenith angle was 25.75°.

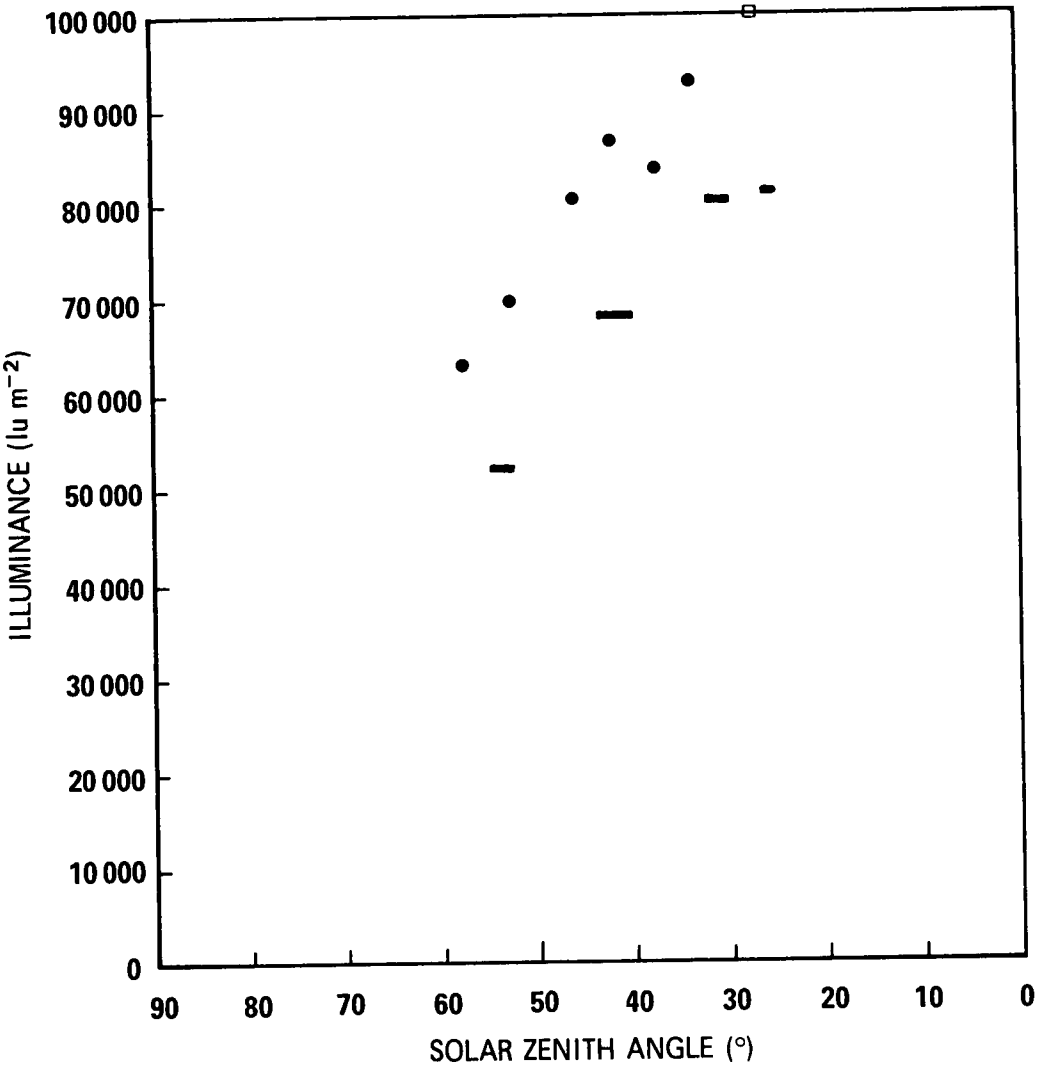

Fig. 21. Downwelling illuminance E(2070, −) as a function of solar zenith angle. The data indicated by the filled circles are those recorded by ground based irradiometer, the elongated data points are from extrapolated aircraft irradiometer data, and the open box □ from spectroradiometric data weighted by the luminance efficiency function, recorded at the surface of Crater Lake. The ground station location was at an altitude of 2070 m. The surface of Crater Lake is at an altitude of 2020 m.

ATMOSPHERIC OPTICAL MEASUREMENTS IN THE VICINITY OF CRATER LAKE, OREGON

Part 2

Almerian R. Boileau

ABSTRACT

This report, Part II, presents additional atmospheric optical data, comparable to the data presented in Part I, but for a different type of day, and for four descents instead of two. Three of the descents were before local apparent noon; the fourth descent was after local apparent noon. Simultaneous spectral irradiance data were recorded at the surface of Crater Lake. Data presented are altitude profiles of heading of aircraft, temperature, relative humidity, equilibrium luminance, horizontal path function, attenuation length, nadir luminance, upwelling and downwelling illuminances and their ratios, reflectance calculated from nadir luminance, atmospheric beam transmittances for vertical path of sight as a function of solar zenith angle, and downwelling illuminance as a function of solar zenith angle.

INTRODUCTION

This report presents atmospheric optical and meteorological data recorded in the vicinity of Crater Lake, Oregon, on the third day of a three day period, 2-4 August 1966. On this day data were recorded nearly simultaneously (1) in an Air Force C-130 aircraft flying over Crater Lake, (2) at a ground station set up on the southern slope of Mt. Mazama, in the caldera of which Crater Lake is located, and (3) on the surface of Crater Lake itself.[1,2] The data reported herein are of the same type as reported in Part I of this report and as published in a series of journal papers.[3-7]

This report is the final report under U. S. Navy Ship Systems Command Contract NObsr-95251, Task II.

Work in this same general area is being continued under Air Force Contract No. F19628-67-C-0181.

THE FLIGHT

The instrumented aircraft, Air Force C-130, No. 022, took off from Kingsley Field, Klamath Falls, Oregon, at 0833* and arrived over Crater Lake at 0910. At the time of takeoff the sky was clear of clouds. The dry air temperature was 20°C, the atmospheric pressure was 879 mb, and the relative humidity was 60%.

Four level-attitude data gathering descents were made, alternately in northerly and southerly directions. The first descent was started from south of Crater Lake, from an altitude of 8000 m, at 0923, and ended north of the lake, at an altitude of 2700 m, at 0937. The second descent was a southerly descent from 8000 m, at 1025, to 1400 m, at 1046. Between these two descents, at about 0940, clouds were forming near the 2800 m altitude. The third and fourth descents were northward from 8000 m, at 1145, to 2200 m, at 1202, and southward from 8800 m, at 1254, to 2500 m, at 1313. Local apparent noon occurred between the third and fourth descents, at approximately 1215.

During the time that data were being recorded in the C-130 aircraft, atmospheric optical data were also being recorded at the ground station, and spectroradiometric data were being recorded at the surface of Crater Lake.

DATA

The magnetic heading of the aircraft during the four descents is shown in Fig. 1. The altitude profiles of dry air temperature and relative humidity are shown in Figs. 2 and 3. The altitude of the aircraft, plotted as a function of elapsed time, for each of the four descents, is shown in Fig. 4.

Atmospheric optical data profiles are shown in Figs. 5 through 21. Fig. 5 shows the four equilibrium luminance profiles in two groupings, the profiles for the two northerly descents being shown in the left side of the figure, the profiles for the two southerly descents being shown on the right. The four horizontal path function profiles are presented in Fig. 6. These are grouped in the same manner as the equilibrium luminance profiles in Fig. 5, that is, the profiles for the northerly descent are shown on the left, profiles for the southerly descent are shown on the right. Figs. 7 through 10 show the profiles of attenuation length and equivalent attenuation length for the four descents.

The nadir luminances for the four descents are shown in Figs. 11 through 14. There is very little similarity in these four profiles. This, of course, is because a terrain of varying texture and reflectance was being seen by a telephotometer having a 5° circular field. The one thing common to the four profiles is the distinct change of nadir luminance as the aircraft passed over Crater Lake. There was no observable sun glitter, observable, that is, by the nadir telephotometer, on the surface of the lake during the first two descents. Glitter was observed during the third and fourth descents.

Fig. 15 shows the downwelling and upwelling illuminances for the first and third descents. Fig. 16 shows the same quantities for the second and fourth descents. The increase in downwelling illuminance with increase in solar zenith angle is greater than the cosine effect of the flat plate collector. This fact, coupled with reduction of beam transmittance, for the vertical path of sight with decrease of solar zenith angle (see Fig. 20), is interpreted as showing that there was an increase in atmospheric scattering,

* Pacific Daylight Time is used throughout this report.

with a consequent increase in the zenith and near zenith sky luminance values. These sky luminances, being near the zenith, cause a larger increase in the value of illuminance on a horizontal flat plate collector than the effect due to the cosine of the change in zenith angle.

The profiles of reflectance, ratios of upwelling to downwelling illuminances, are shown in Fig. 17. These have been grouped by the direction of the descent, the profile of the northerly descents being on the left and the profiles of the southerly descent being on the right. For comparison, reflectance profiles calculated from nadir luminance and downwelling illuminance are presented in Figs. 18 and 19. These profiles also are grouped by direction of the descents. Also, these profiles, resulting from data measured with a telephotometer having a 5° field, have much more structure than the ratio of illuminance profiles.

Fig. 20 is a plot of beam transmittances for the vertical path of sight, from 2070 m to space, as a function of the solar zenith angle.

Fig. 21 is a plot of the various values of downwelling illuminance at the 2070 m level as the solar zenith angle changes. These data were obtained from three sources: ground-based irradiometer measurements, extrapolated airborne irradiometer measurements, and calculations based on the spectroradiometric data measured at the surface of the lake.

ACKNOWLEDGEMENTS

Visibility Laboratory personnel during this field trip were: R. W. Johnson, Senior Development Engineer, supervising personnel of the Atmospheric Research Branch; G. C. Barnett, Assistant Development Engineer, responsible for the airborne activities; K. W. McMasters, Senior Electronics Technician, and R. L. Sydnor, Senior Laboratory Mechanician, assisting Mr. Barnett in the aircraft; and G. F. Simas, Senior Electronics Technician, assisting Mr. Johnson at the ground station; R. C. Smith, Assistant Research Physicist, of the Underwater Optical Research Group, operating the spectroradiometer at the surface of Crater Lake; and J. J. Lones, Associate Development Engineer, Engineering Branch, assisting Dr. Smith.

The crew of the C-130 aircraft consisted of Capt. Paul Griswold, USAF, Aircraft Commander; 1st Lieut. Roger Lowther, USAF, pilot; Sgt. Castro, crew chief, and Airman LaRossa. Their fullest cooperation in flying the aircraft in the requested flight pattern was much appreciated.

Many members of the Crater Lake Park staff assisted in this field trip, and their assistance is gratefully acknowledged. Ranger John Chapman was especially helpful in assisting Mr. Johnson in his selection of a site for the ground station.

REFERENCES

1. R. C. Smith and J. E. Tyler, J. Opt. Soc. Am. **57**, 589 (1967).
2. J. E. Tyler and R. C. Smith, J. Opt. Soc. Am. **57**, 595 (1967).
3. S. Q. Duntley, **et al**, Appl. Opt. **3**, 549 (1964).
4. J. I. Gordon and P. V. Church, Appl. Opt. **5**, 793 (1966).
5. A. R. Boileau and J. I. Gordon, Appl. Opt. **5**, 803 (1966).
6. J. I. Gordon and P. V. Church, Appl. Opt. **5**, 919 (1966).
7. A. R. Boileau, Appl. Opt. **7**, 407 (1968).

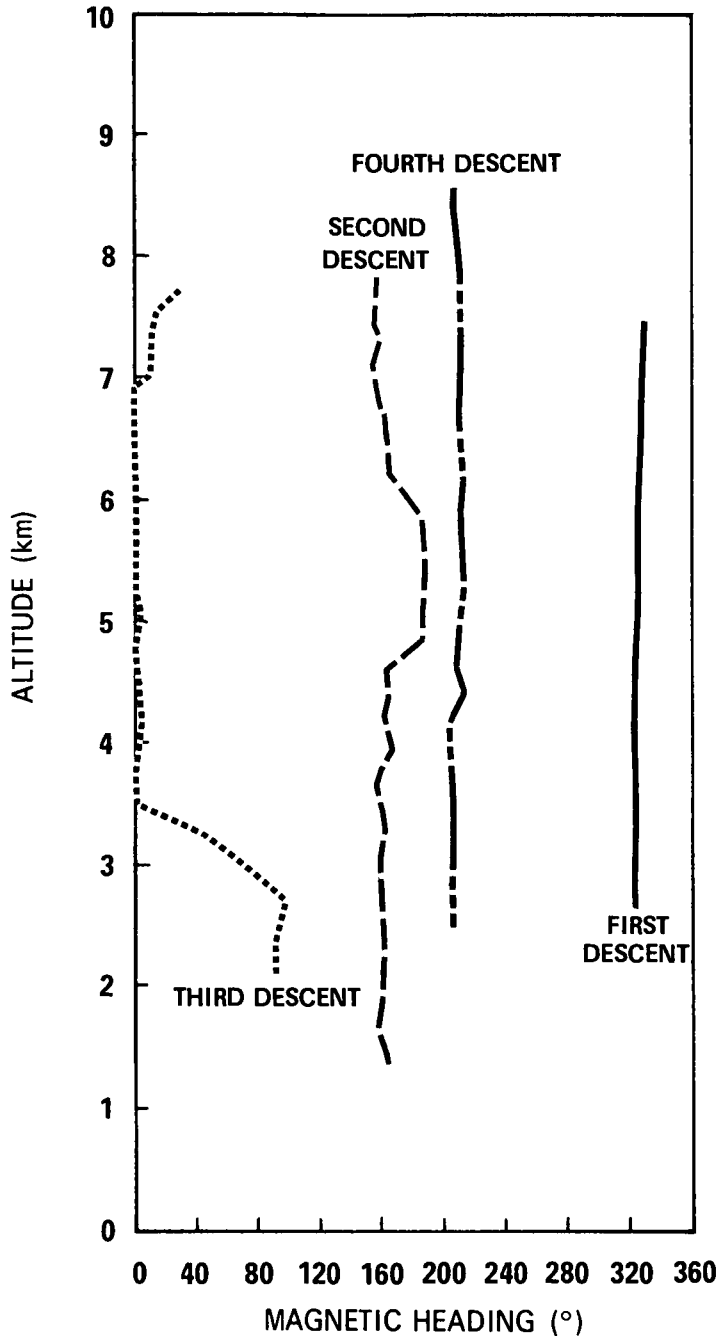

Fig. 1. Aircraft heading, magnetic, during descents. True heading is magnetic heading plus 20°. The change of heading at 6200 m during second descent was made in order to cross the center of Crater Lake; the change at 4900 m was made in order to resume original heading. During the third descent it became necessary to change aircraft heading at 3400 m to avoid clouds.

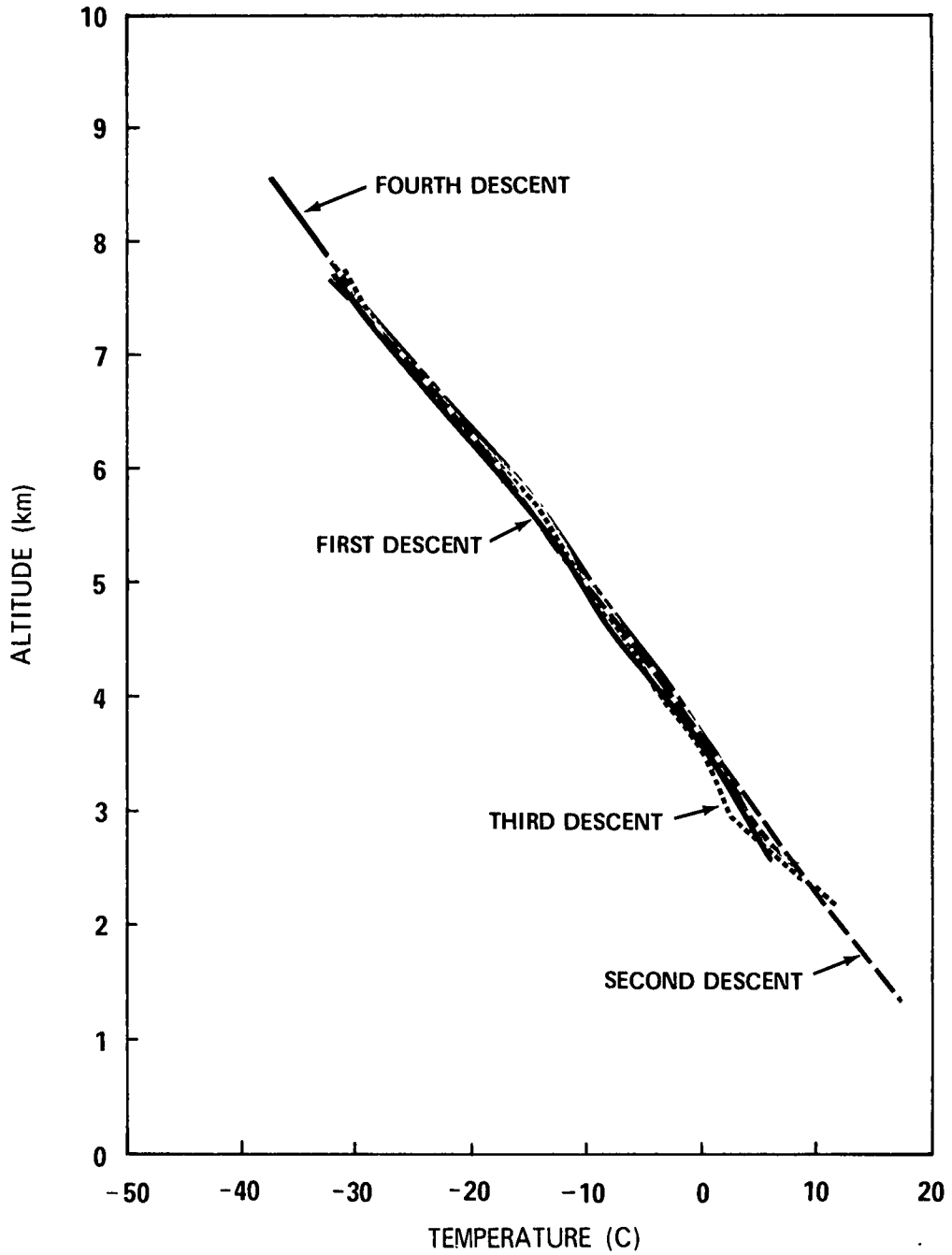

Fig. 2. Altitude profiles of dry air temperature. Only minor changes in these profiles, which are of little significance, occurred during the nearly four hours elapsed time between the start of the first descent and the termination of the fourth descent.

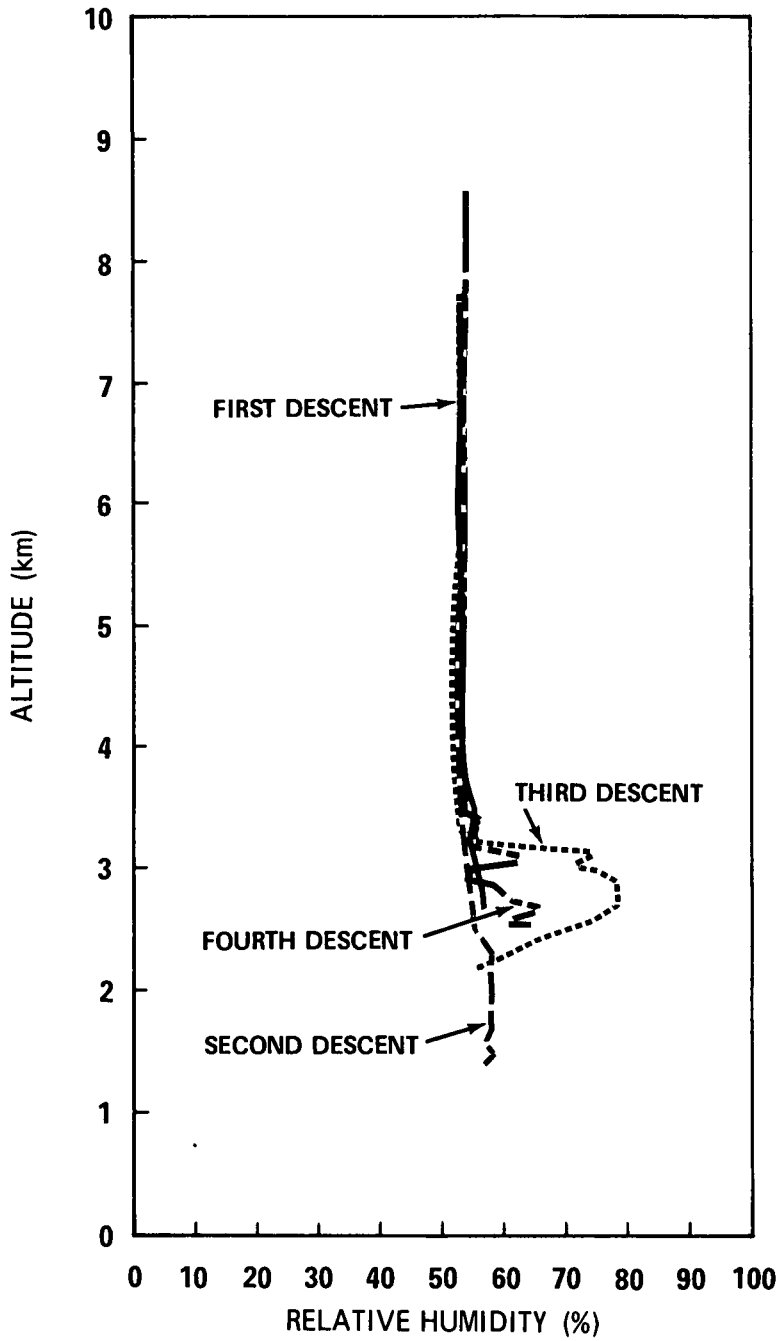

Fig. 3. Altitude profiles of relative humidity. These profiles show no change in relative humidity during the time of the four descents except for the stratum between 3250 m and 2250 m. The relative humidity in this stratum has its greatest measured value at about 1200, before local apparent noon (1215), and then has a lesser value by 1300.

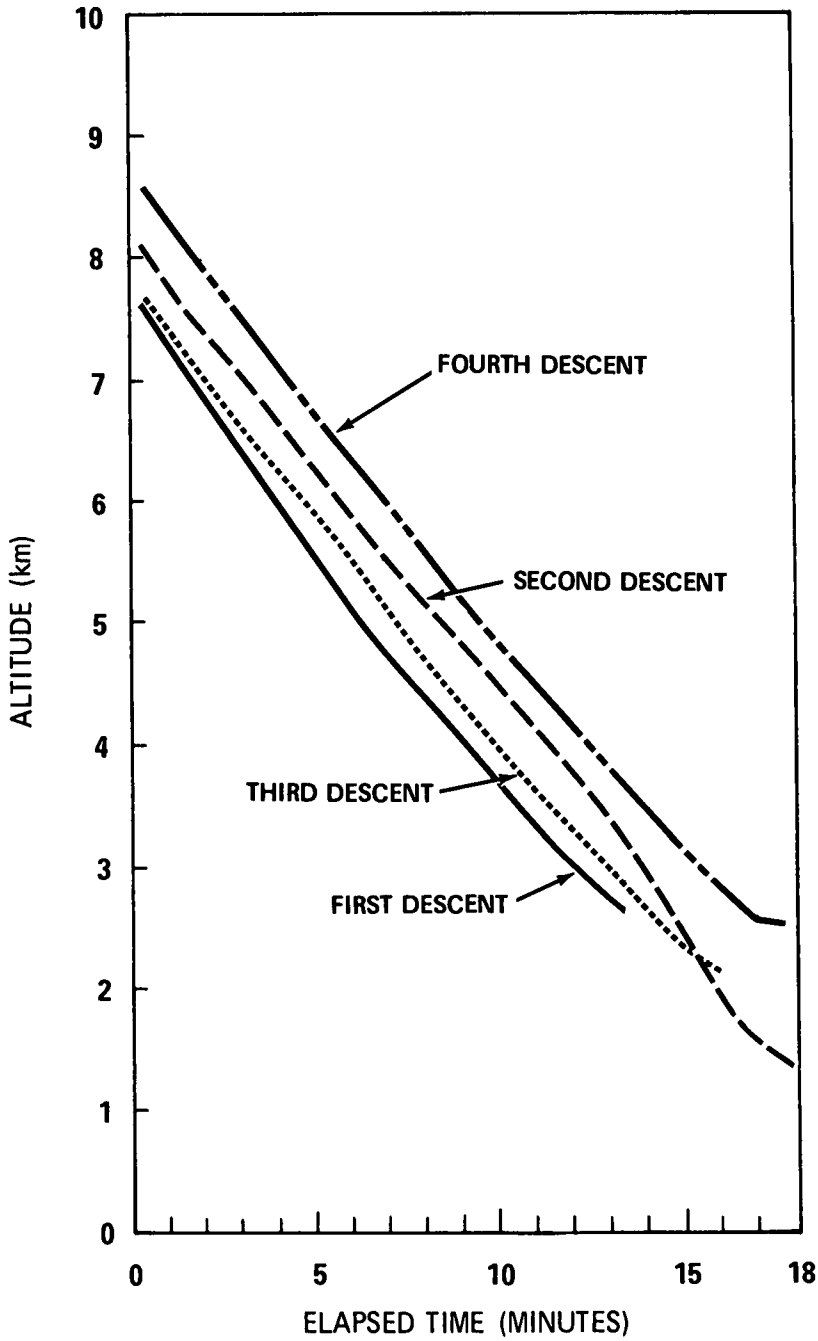

Fig. 4. Aircraft altitude as a function of time during the four descents. Changes in the attitude of the aircraft during descent can be inferred from these plots. It appears that the attitude of the aircraft remained virtually unchanged once a descent was started.

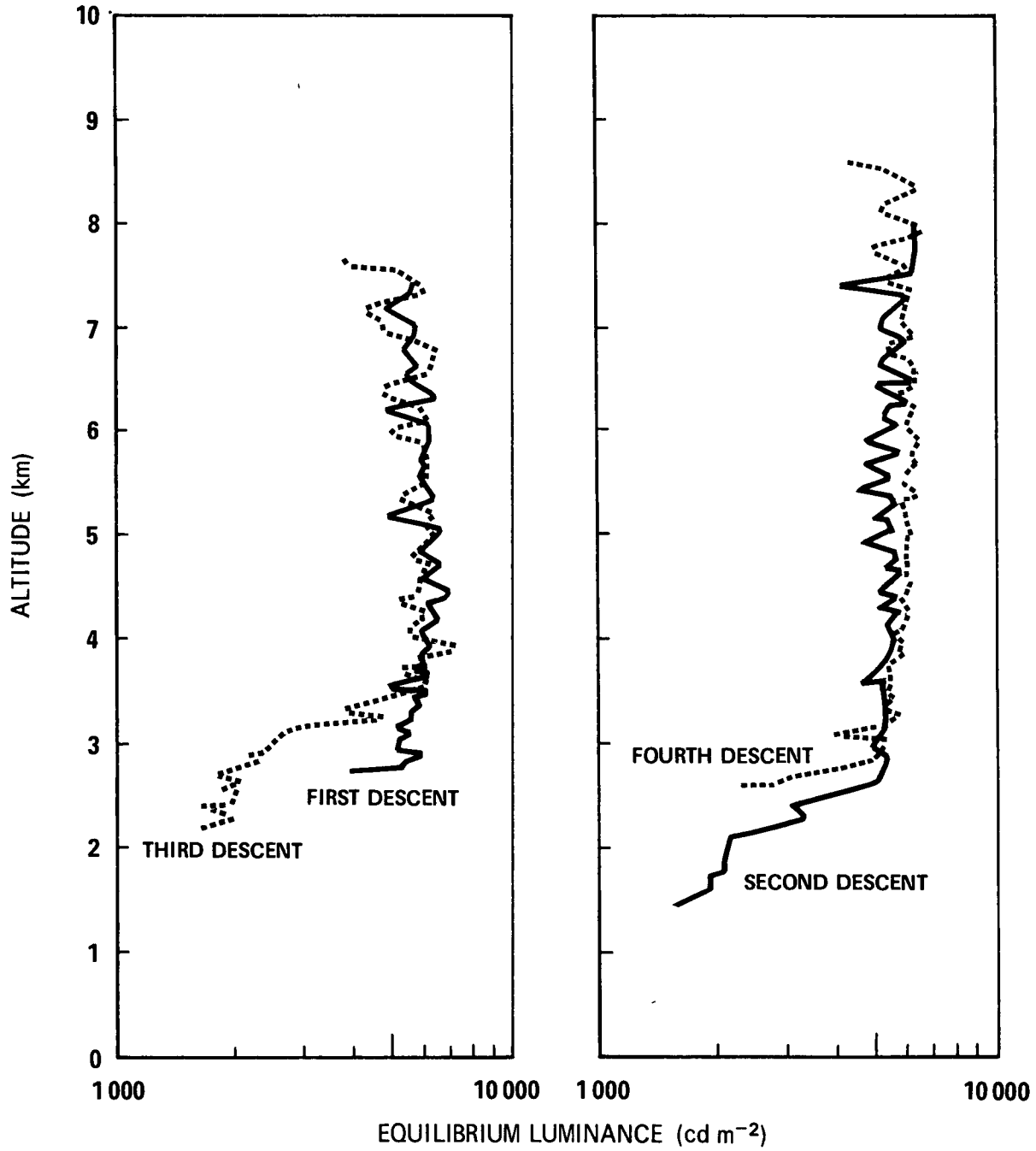

Fig. 5. Profiles of equilibrium luminance $B_q(z, 90°, \phi)$. The values of ϕ for the four descents were 133°, 46°, 148°, and 22°. The random fluctuations with altitude are believed to be spurious with the true equilibrium luminance profiles being approximated by the envelopes of the maximum values. There seems to be no discernible change due to the various values of ϕ.

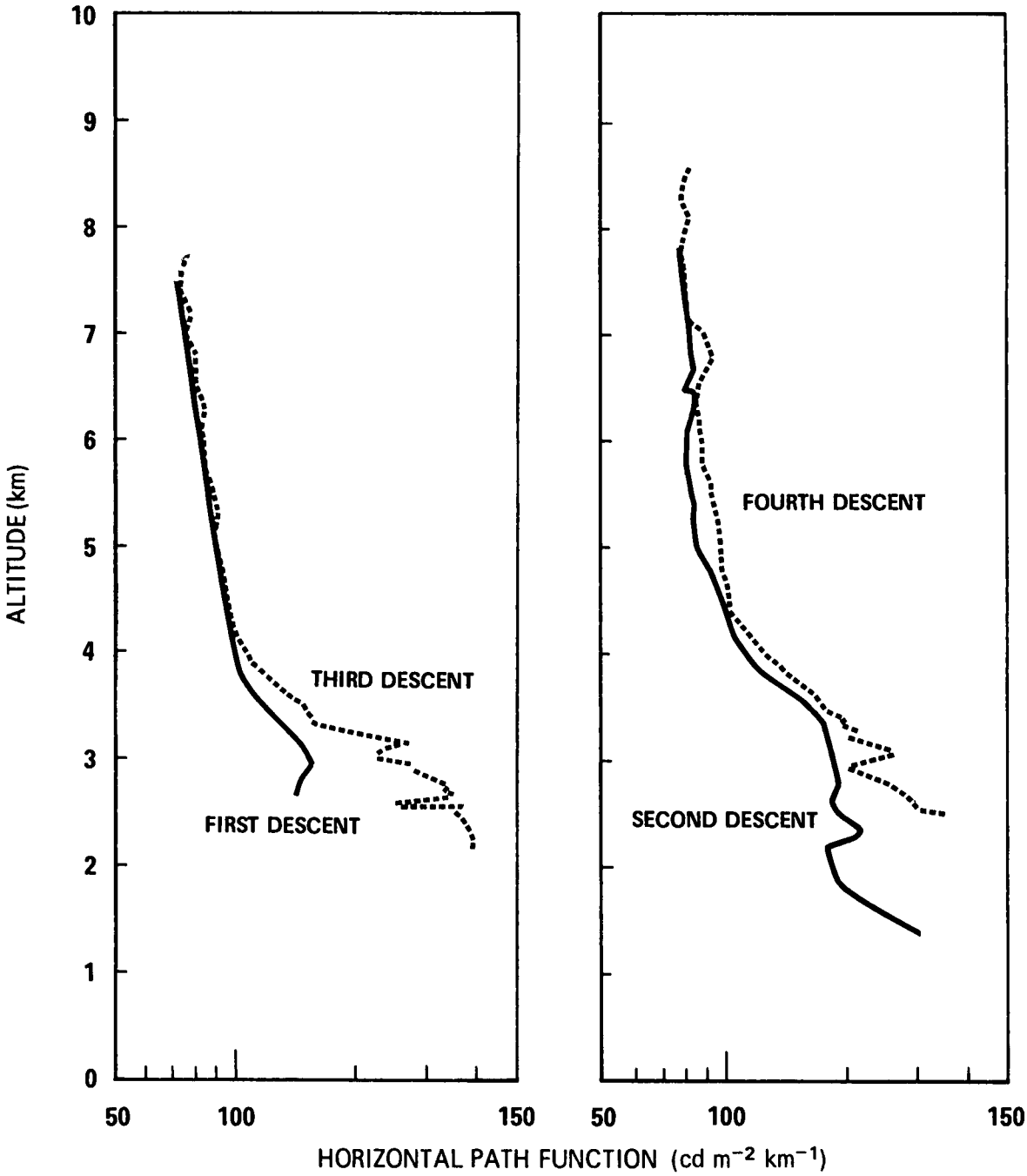

Fig. 6. Profiles of horizontal path function $B_*(z, 90°, \phi)$. The four values of ϕ for the four descents are the same as listed for $B_q(z, 90°, \phi)$, Fig. 5. The large change in the value of $B_*(z, 90°, \phi)$ at 3250 m during the third descent is attributed to the relatively large increase of relative humidity measured at that altitude during the same descent.

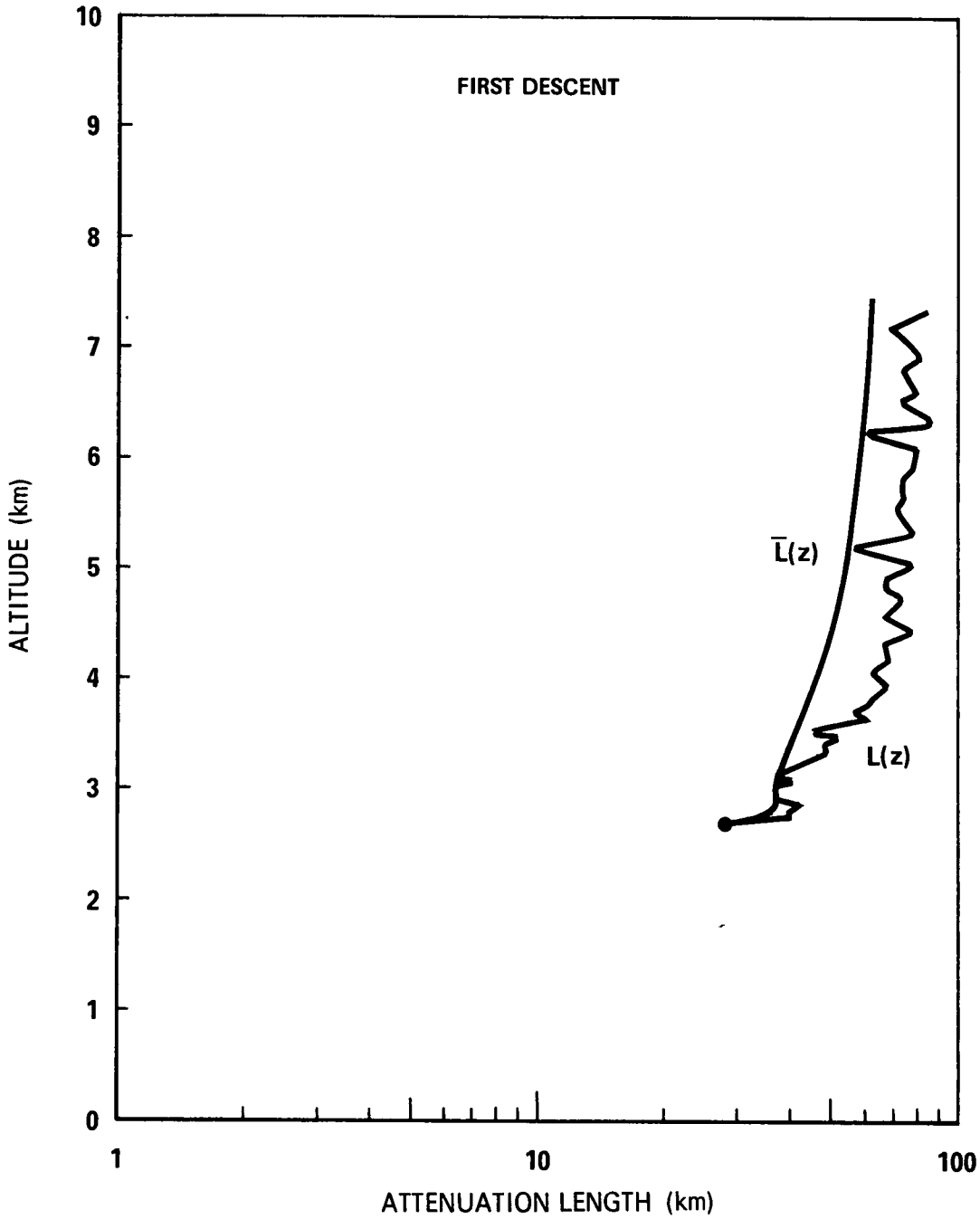

Fig. 7. Profiles of attenuation length L(z) and equivalent attenuation length $\bar{L}(z)$ for the first descent. The random fluctuations in the L(z) profile are primarily due to similar fluctuations of the equilibrium luminance profile.

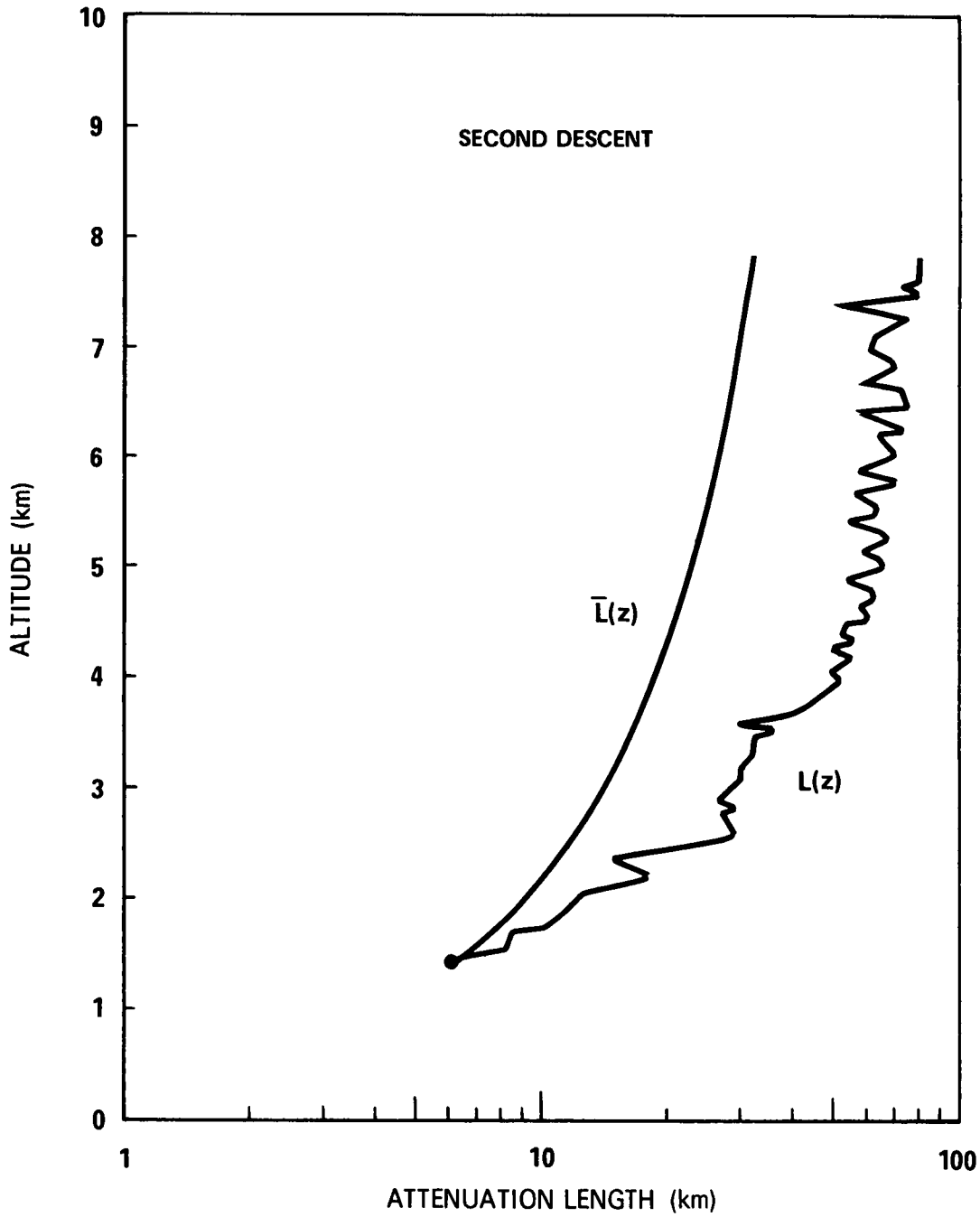

Fig. 8. Profile of L(z) and $\bar{L}(z)$ for the second descent. This profile and the profile of horizontal path function in Fig. 6 show an increase in attenuation in the strata at 3600 m and below.

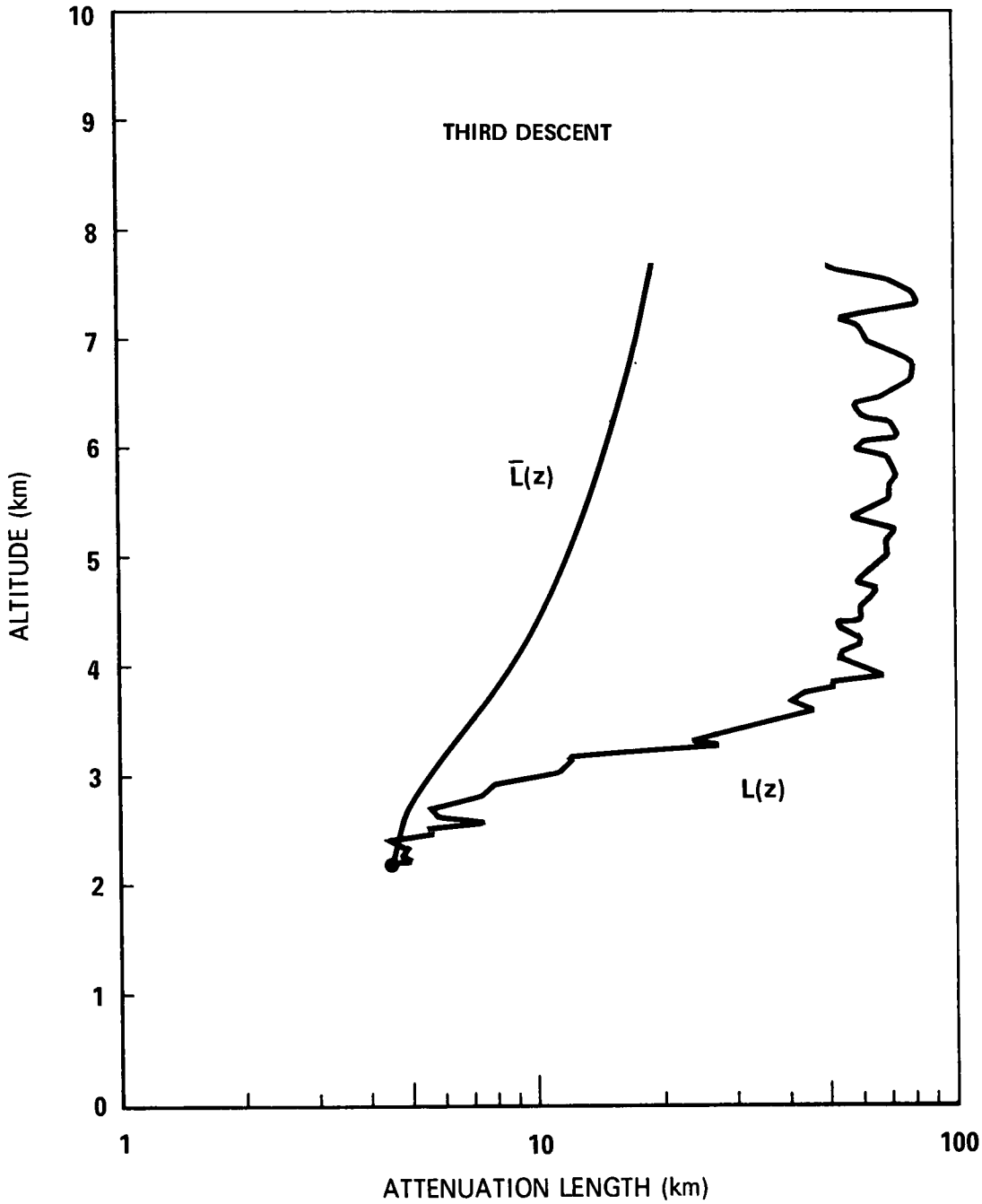

Fig. 9. The third descent profiles for L(z) and $\bar{L}(z)$. A comparison of this profile with that in Fig. 8 shows that the attenuation in the lower altitudes had continued to increase with elapsed time.

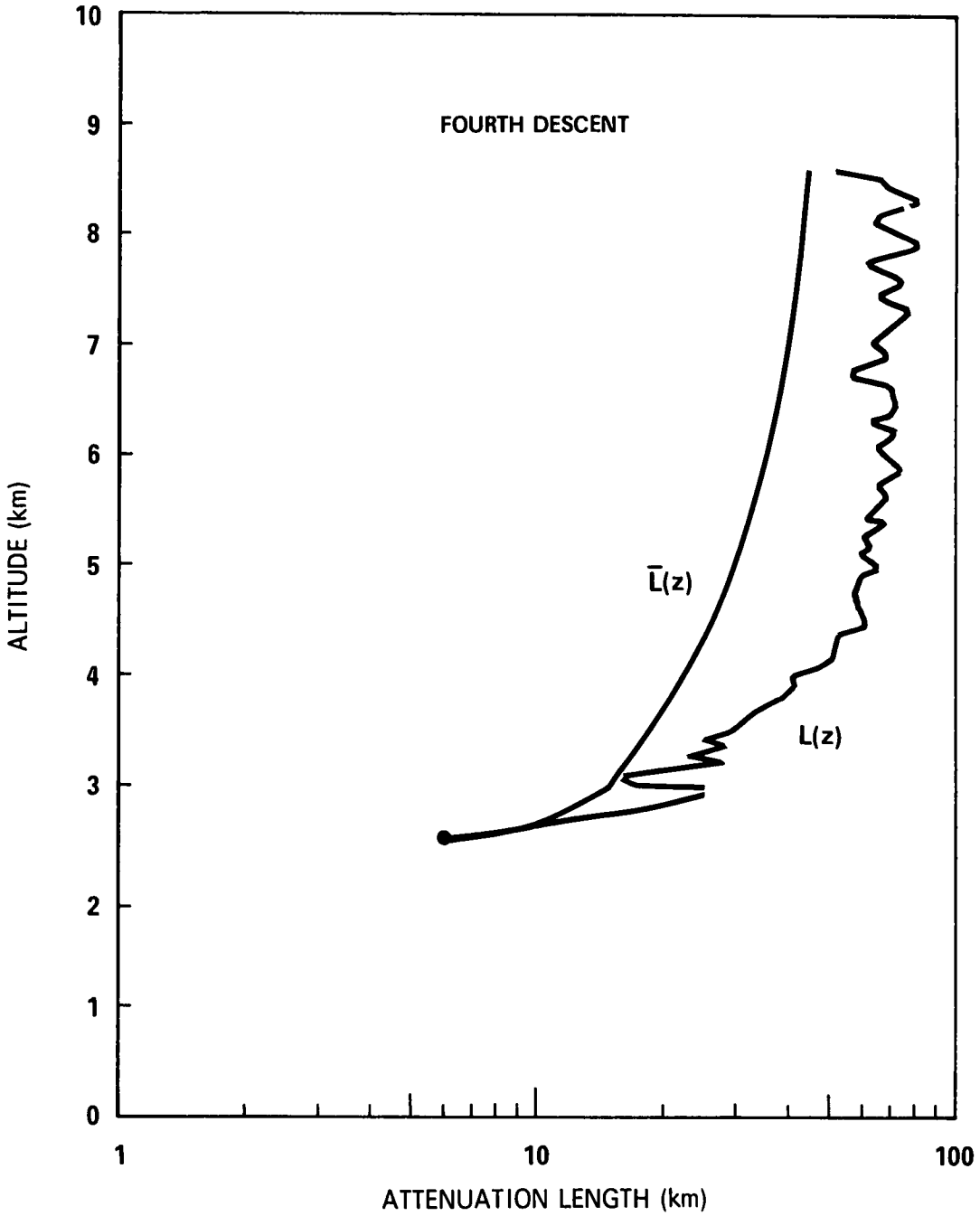

Fig. 10. Attenuation length profiles for fourth descent. The L(z) profile and the $\bar{L}(z)$ profile for the third descent appear to be quite similar, but the transmittance calculated from these profiles (see Fig. 20) show that the transmittance for the vertical path of sight during the fourth descent was higher than the transmittance during the third descent.

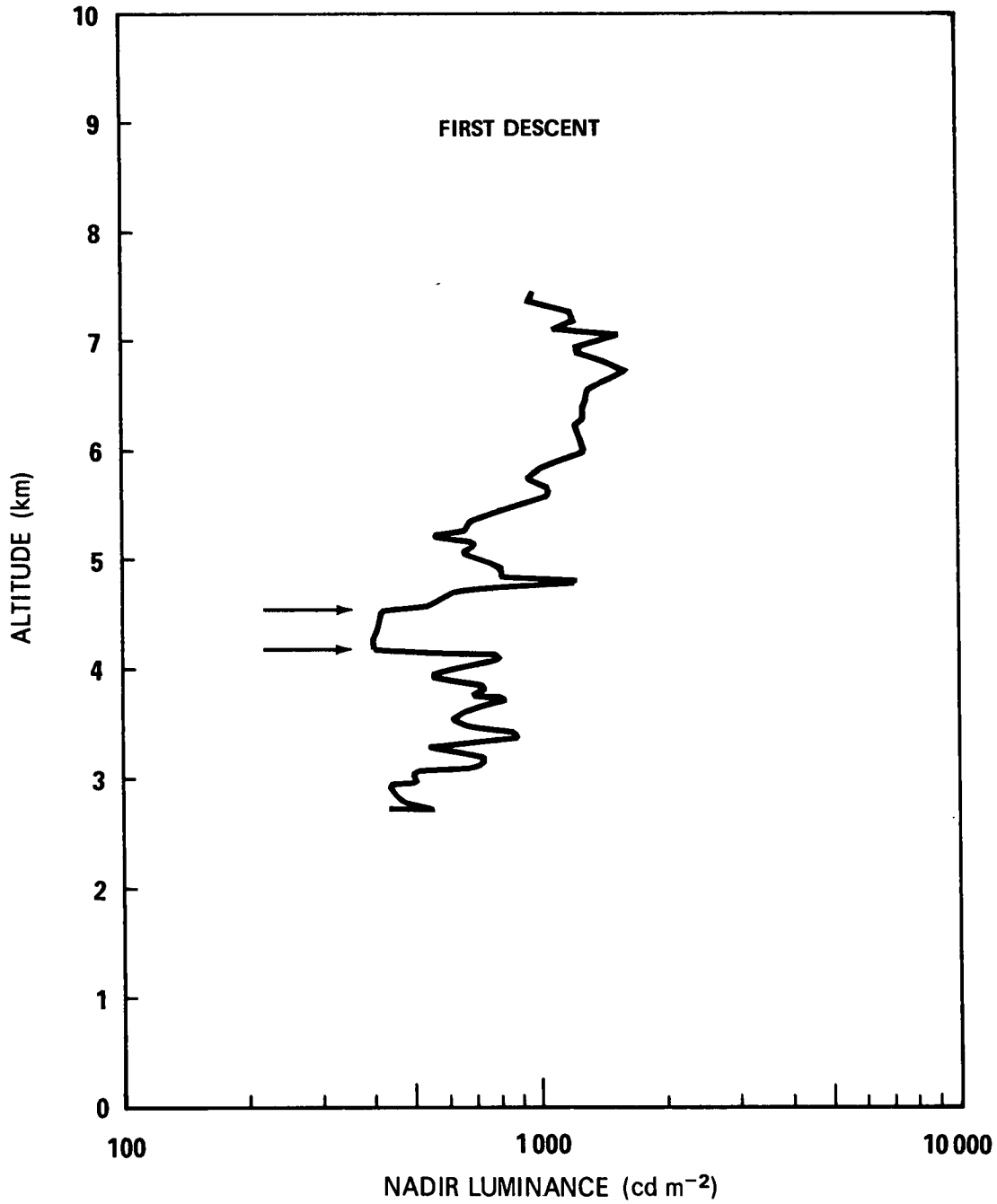

Fig. 11. Nadir luminance $B_r(z, 180°, \phi)$ during first descent. The apparent luminance of Crater Lake during the four descents is that between the arrows in Figs. 11-14.

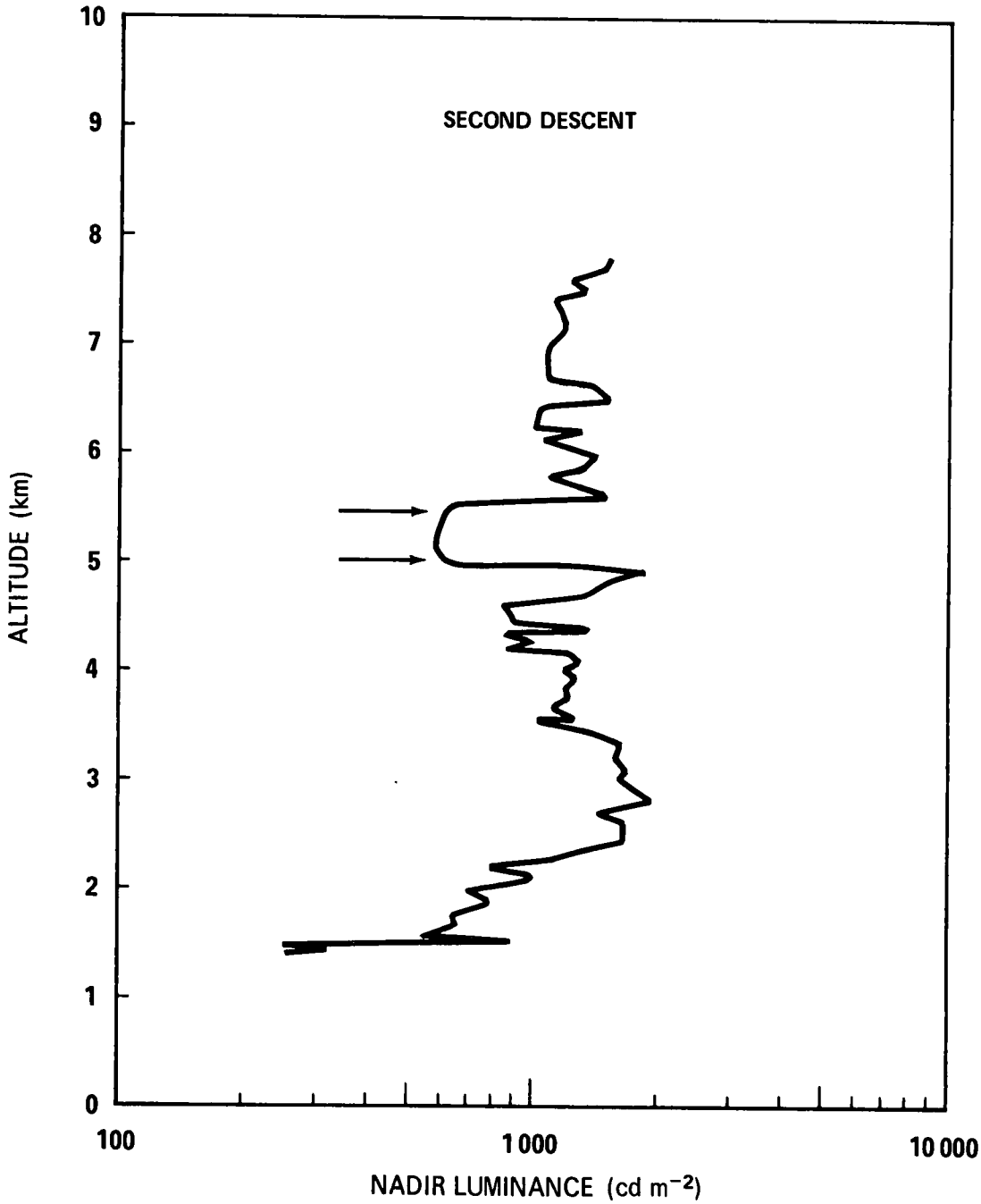

Fig. 12. Nadir luminance during second descent.

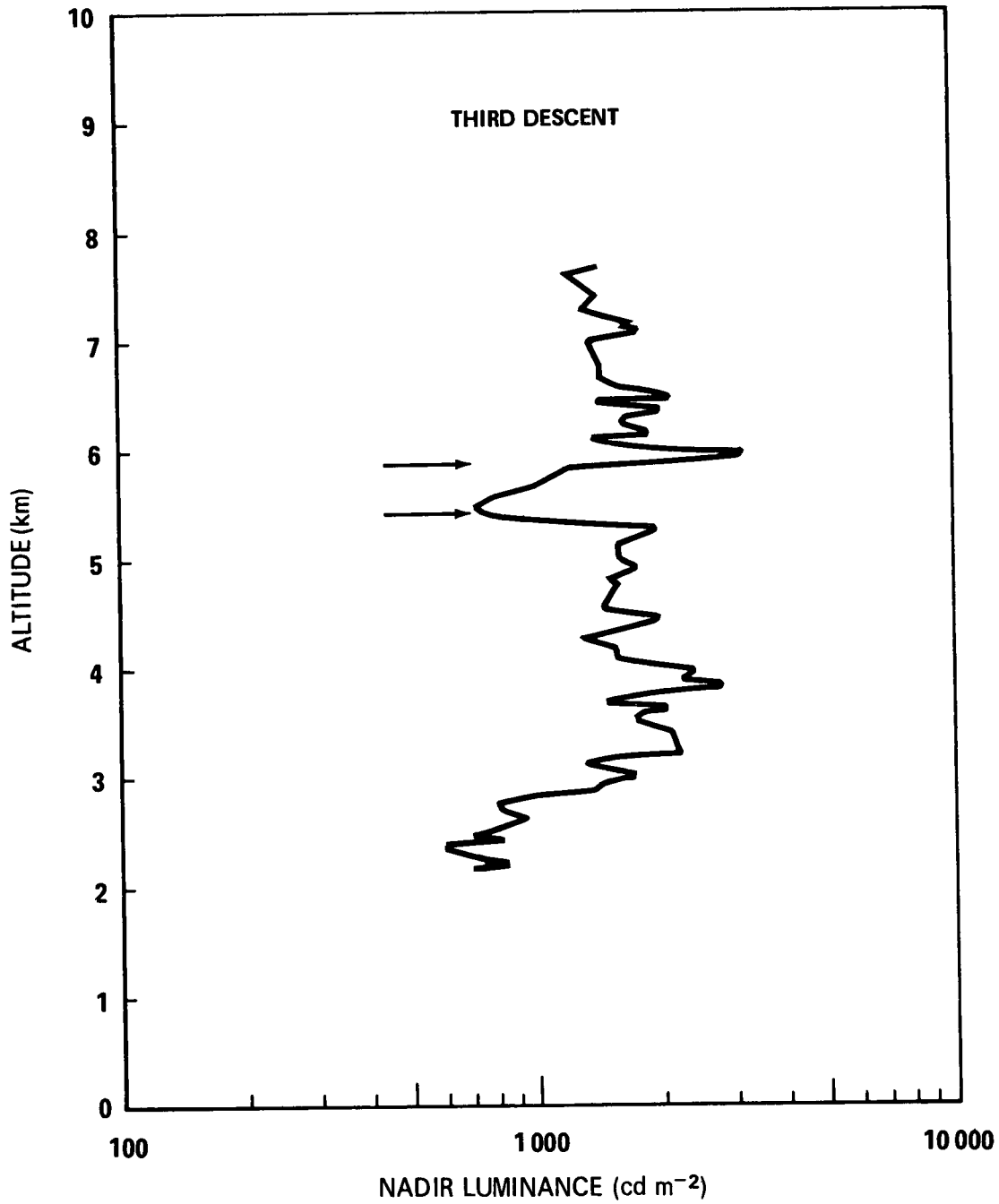

Fig. 13. Nadir luminance during third descent.

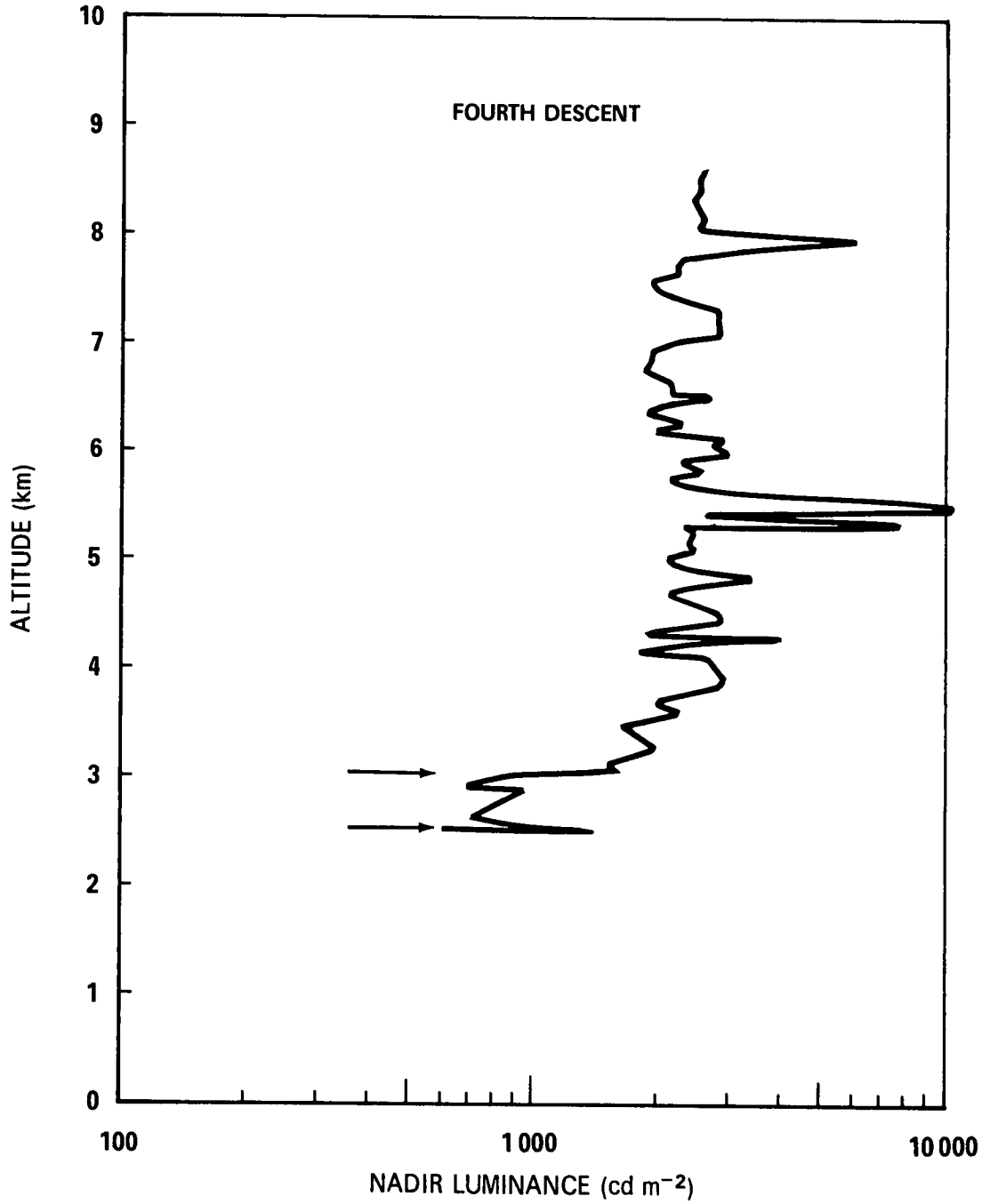

Fig. 14. Nadir luminance during fourth descent.

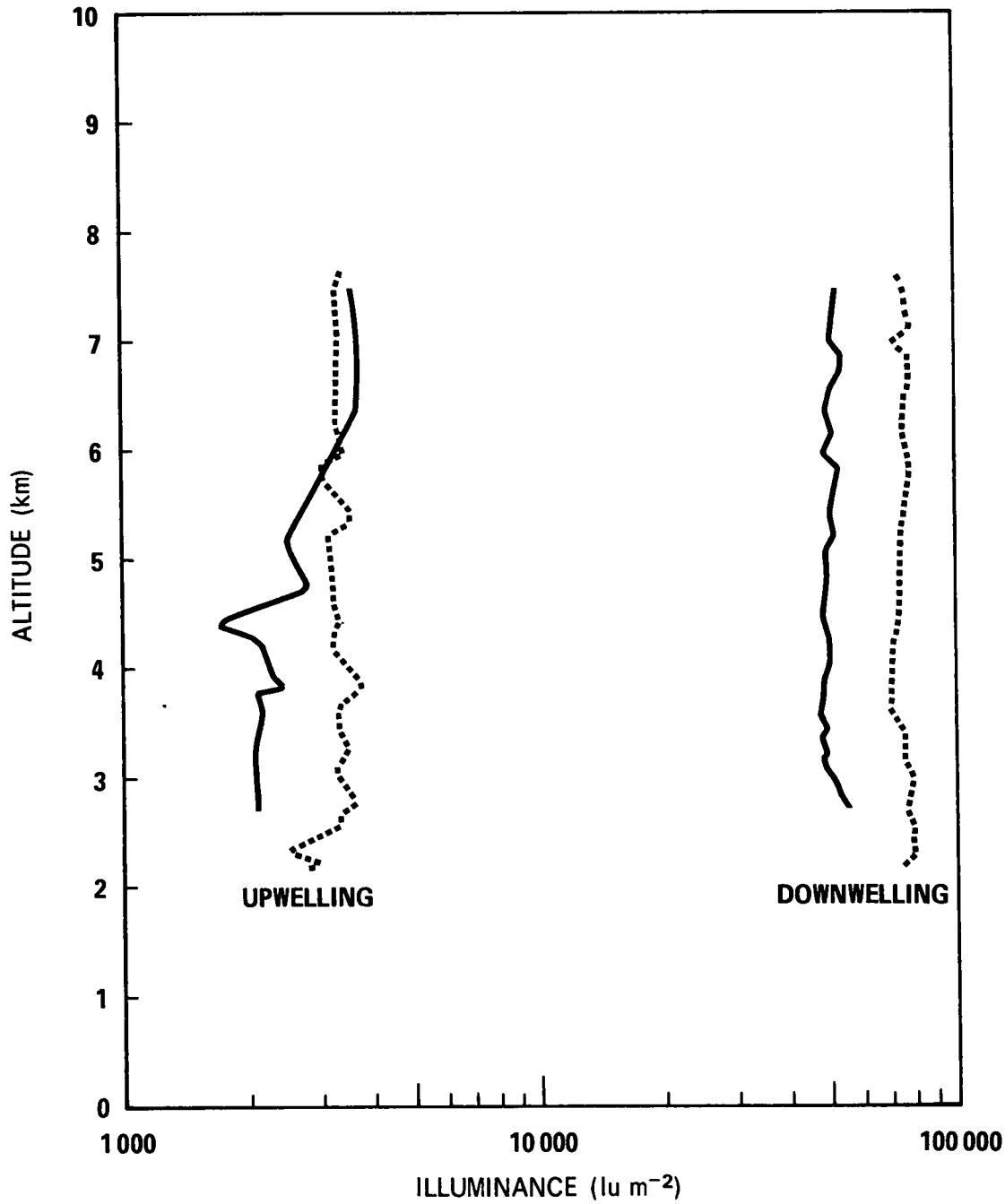

Fig. 15. Downwelling and upwelling illuminances, E(z,−) and E(z,+) respectively, during first and third descents. The solid line profiles are for the first descent, the broken line profiles are for the third descent.

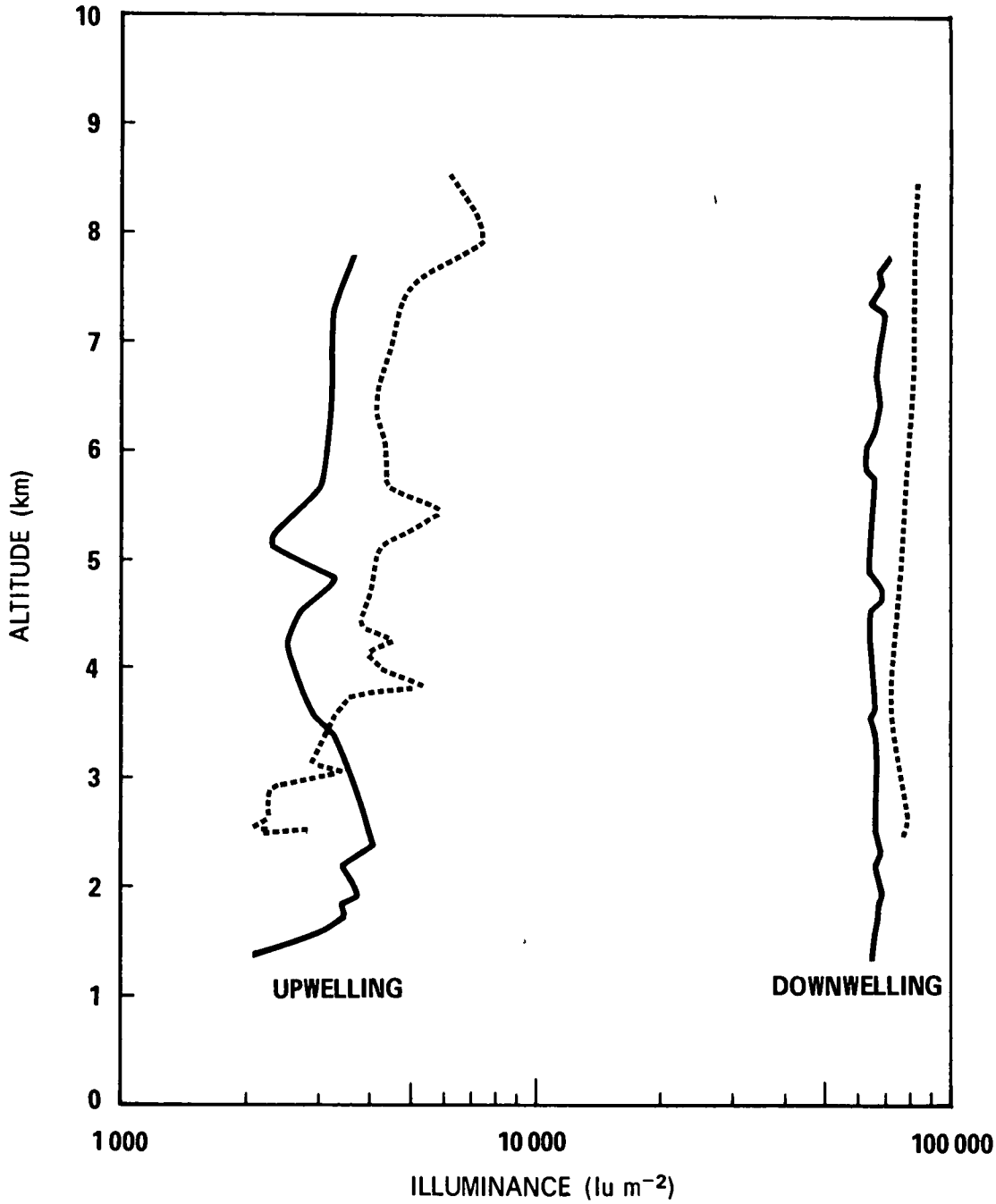

Fig. 16. Downwelling and upwelling illuminances for second and fourth descents. The solid line profiles are for the second descent, the broken line profiles are for the fourth descent.

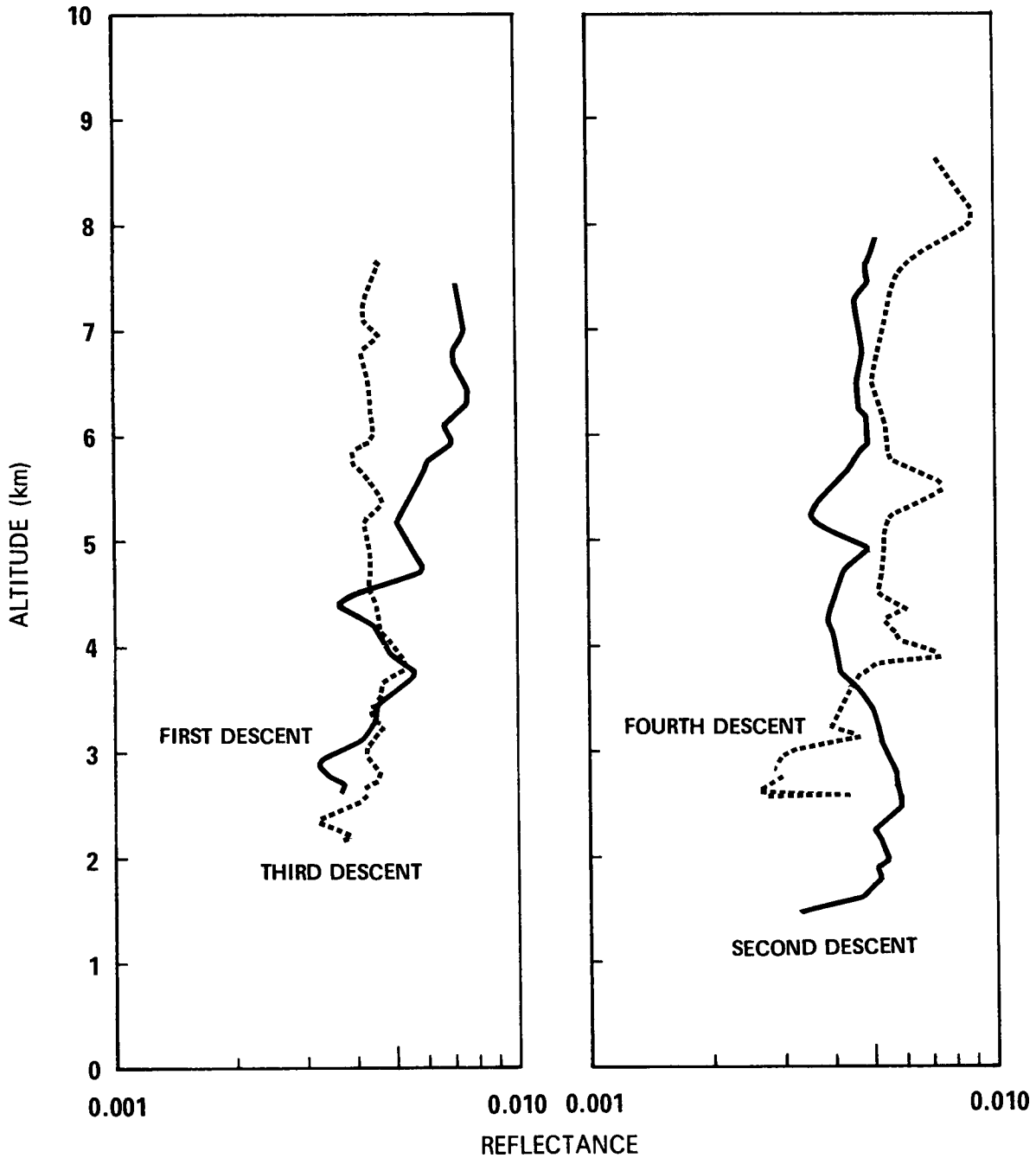

Fig. 17. Profiles of ratios of upwelling and downwelling illuminances during first and third descents and during second and fourth descents. These reflectances are found by the equation

$$R_r(z, 180^\circ, \phi) = E(z,+)/E(z,-)$$

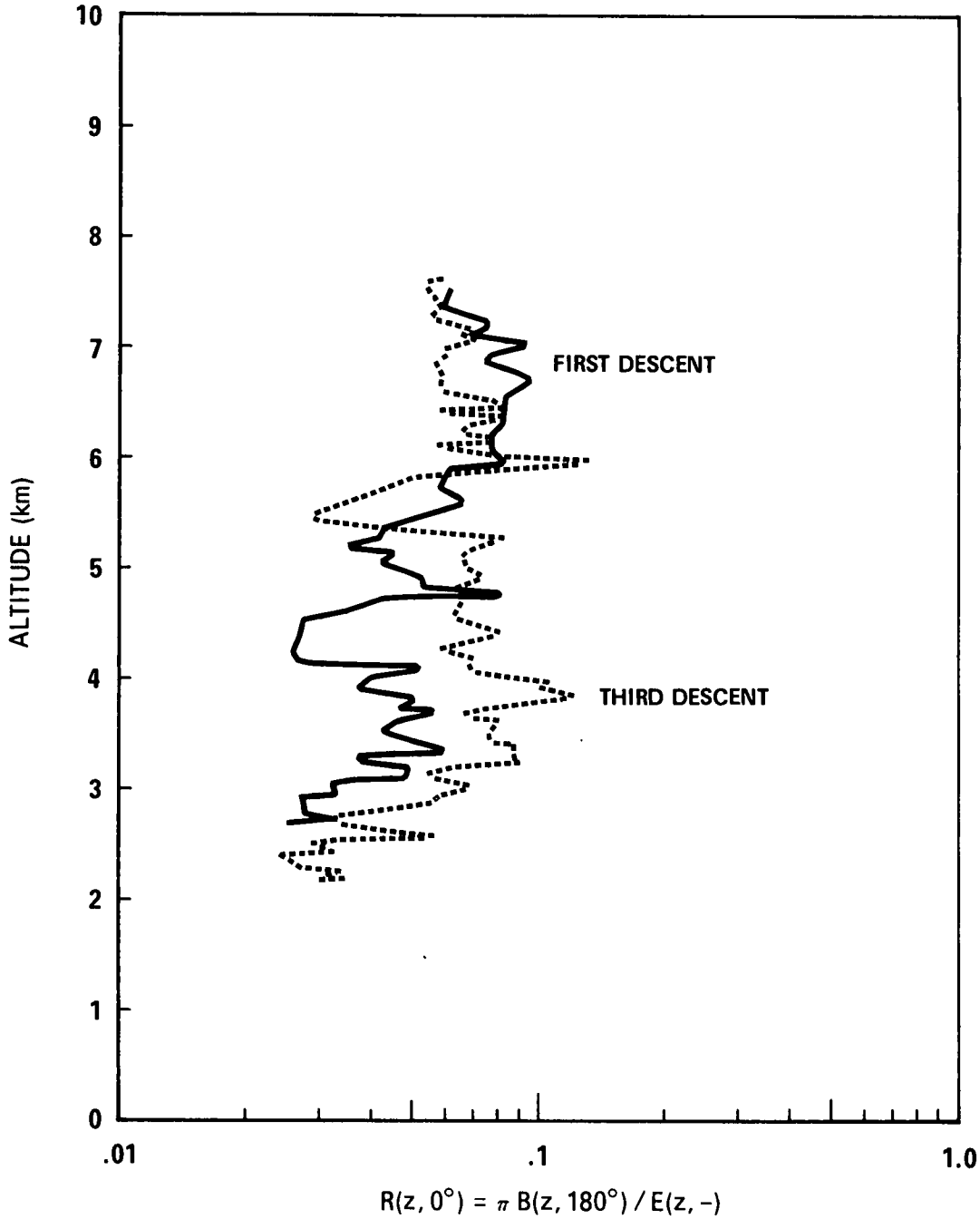

Fig. 18. Profiles of terrain reflectance for first and third descents calculated from nadir luminances and downwelling illuminances by the equation

$$R_r(z, 180°, \phi) = \pi B_r(z, 180°, \phi) / E(z, -)$$

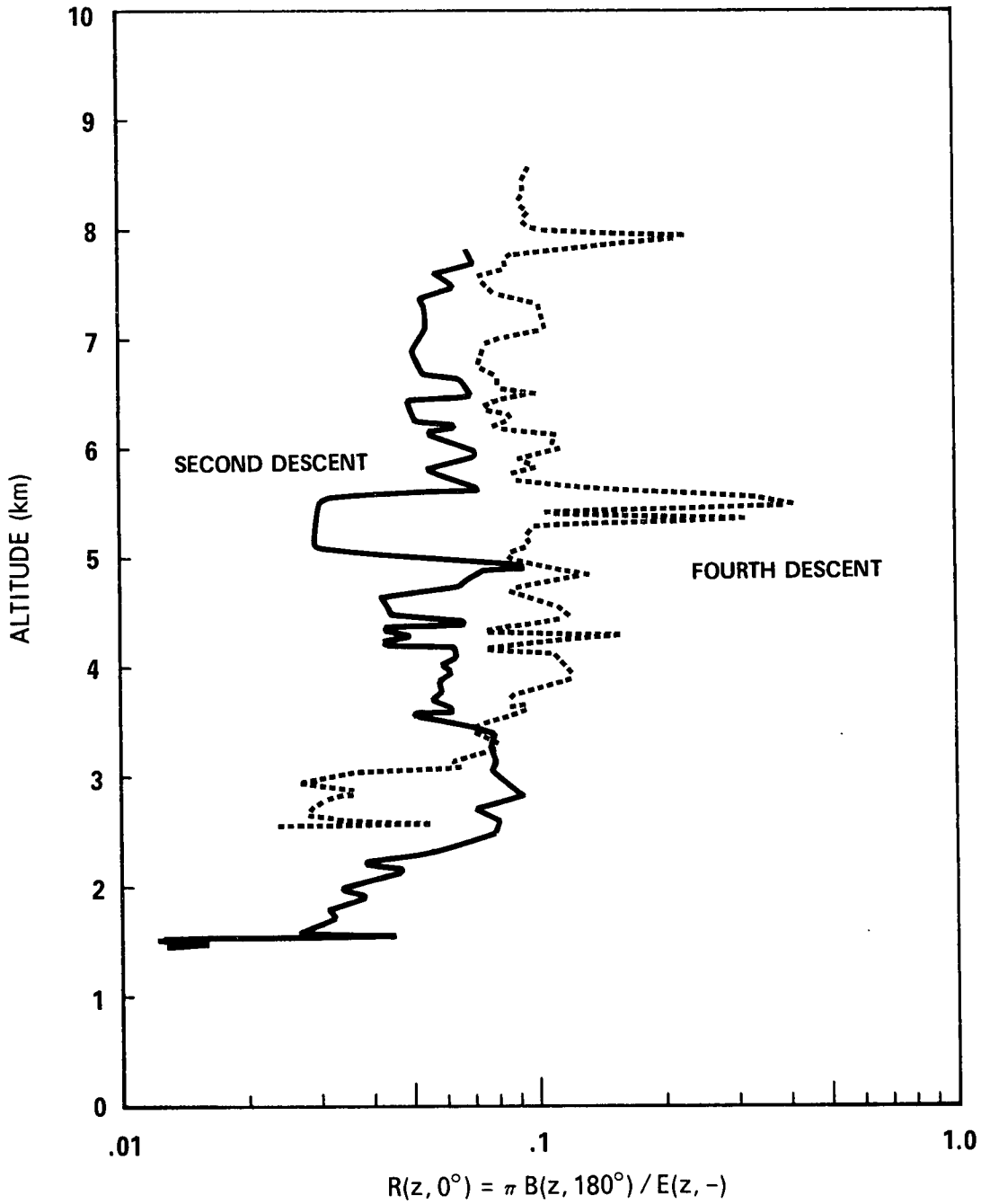

Fig. 19. Profiles of terrain reflectance for second and fourth descents calculated in the same manner as the profile in Fig. 18.

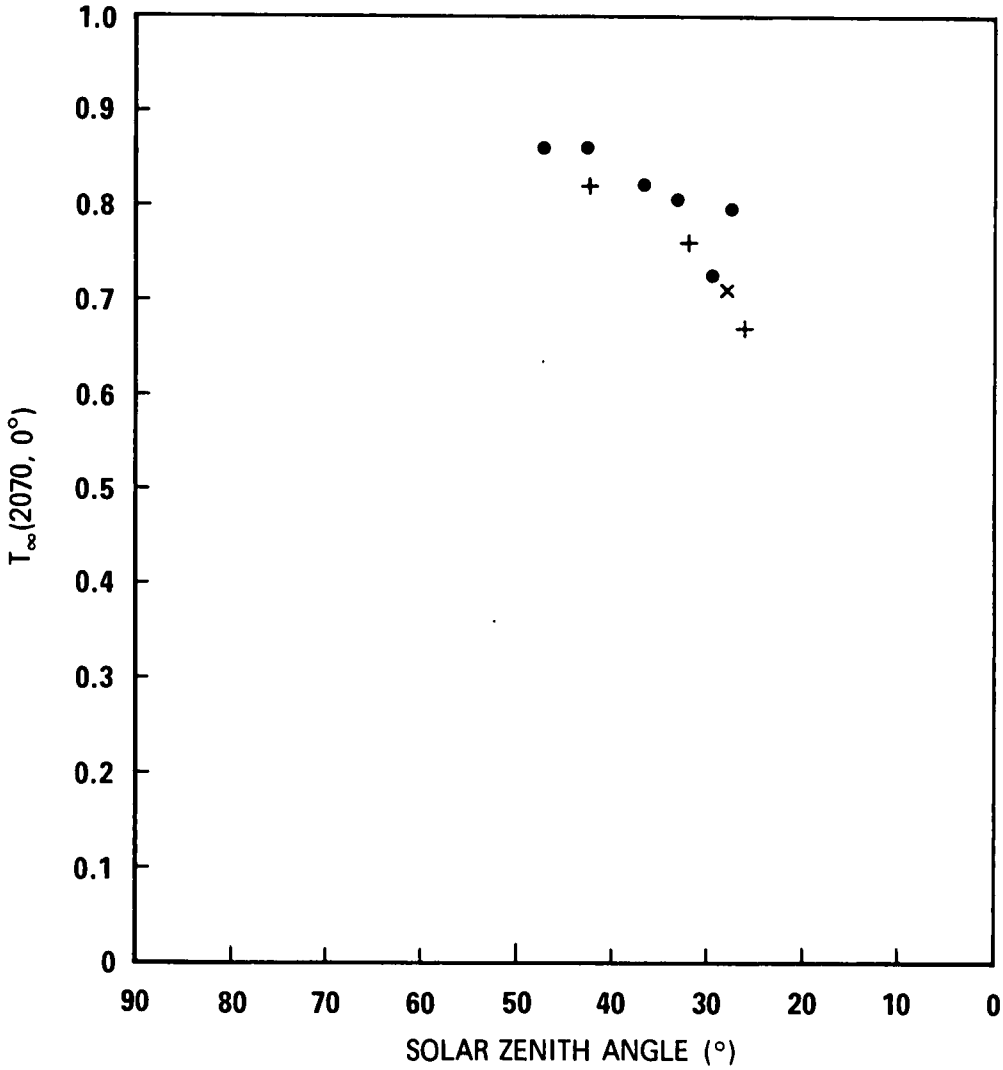

Fig. 20. Beam transmittance for the vertical path of sight as a function of the solar zenith angle. The data shown by filled circles were calculated from ground-based data and the equation

$$T_\infty(2070, 0°, 0°) = \left[\frac{{}_sB_\infty(2070, \theta_s, \phi_s)}{{}_sB_o}\right]^{\cos \theta_s}$$

The data shown by vertical crosses and the x were from extrapolated aircraft data and the equation

$$T_\infty(2070, 0°, 0°) = \exp\left[-\Sigma \Delta z / L(z)\right].$$

The vertical crosses represent forenoon transmittance values, the cross represents the afternoon transmittance value. Note that during the forenoon the beam transmittance for the vertical path of sight decreased as the solar zenith angle decreased and in the afternoon, for the one data point, increased as the solar zenith angle increased. At 1215 (local apparent noon) the solar zenith angle was 25.75°. The lowest transmittance value obtained was that calculated from aircraft data recorded during the third descent, from 1145 to 1202, with an approximate solar zenith angle of 26.2°.

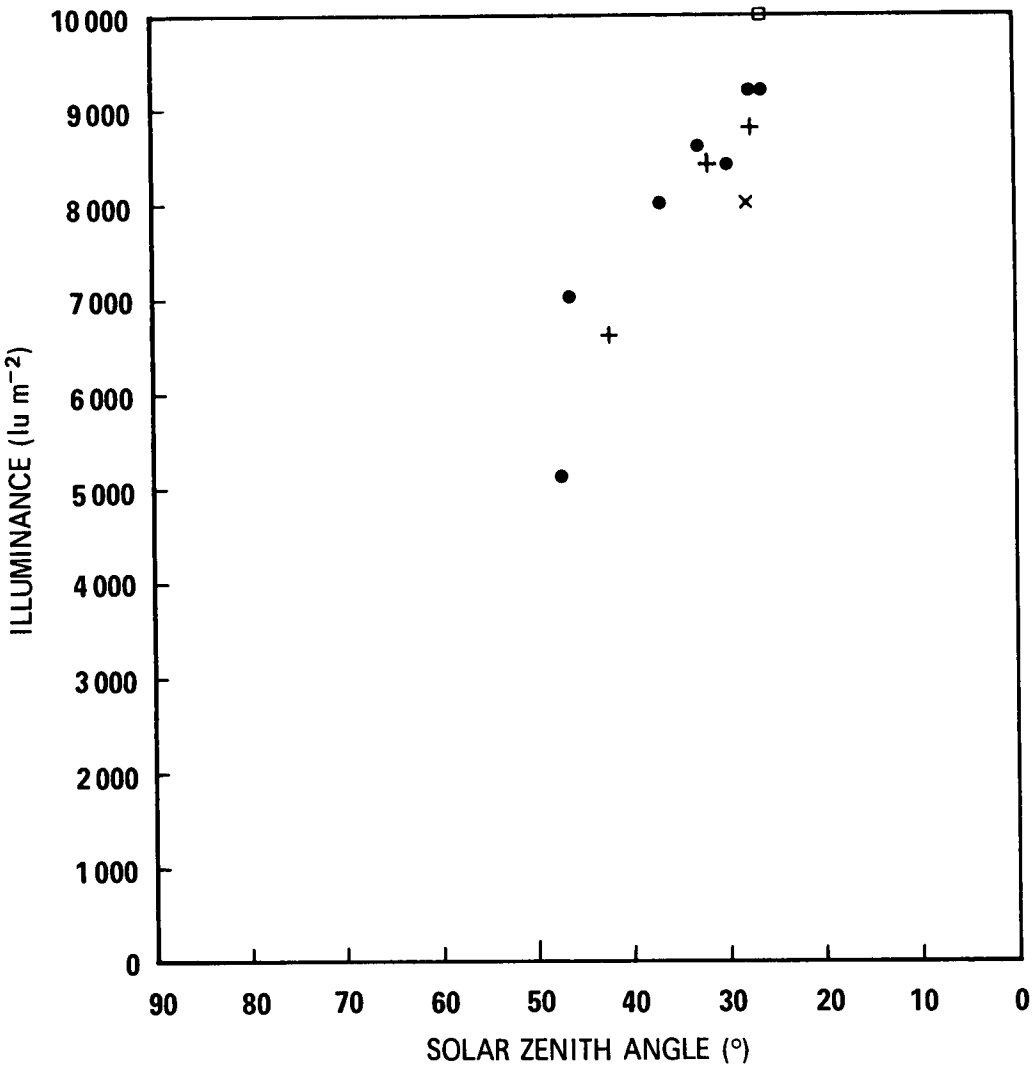

Fig. 21. Downwelling illuminance E(2070, −) as a function of solar zenith angle. The data indicated by the filled circles is that recorded by ground-based irradiometer, the vertical crosses + by extrapolated aircraft irradiometer data recorded during forenoon, the diagonal cross x by aircraft irradiometer data recorded during afternoon, and the open box □ from spectroradiometric data weighted by the luminance efficiency function, recorded at the surface of Crater Lake. The ground station location was at an altitude of 2070 m. The surface of Crater Lake is at an altitude of 2020 m.

UNCLASSIFIED

Security Classification

DOCUMENT CONTROL DATA - R&D

(Security classification of title, body of abstract and indexing annotation must be entered when the overall report is classified)

1. ORIGINATING ACTIVITY *(Corporate author)*

Visibility Laboratory
University of California
San Diego, California 92152

2a. REPORT SECURITY CLASSIFICATION

UNCLASSIFIED

2b. GROUP

3. REPORT TITLE

ATMOSPHERIC OPTICAL MEASUREMENTS IN THE VICINITY OF CRATER LAKE, OREGON. PART II.

4. DESCRIPTIVE NOTES *(Type of report and inclusive dates)*

Final Report

5. AUTHOR(S) *(Last name, first name, initial)*

Boileau, Almerian R.

6. REPORT DATE	7a. TOTAL NO. OF PAGES	7b. NO. OF REFS
June 1968	27	7

8a. CONTRACT OR GRANT NO.	9a. ORIGINATOR'S REPORT NUMBER(S)
NObsr-95251	
b. PROJECT NO.	SIO Ref. 68-19
SF0180301, Task 538	
c. Task II	9b. OTHER REPORT NO(S) *(Any other numbers that may be assigned this report)*
d.	

10. AVAILABILITY/LIMITATION NOTICES

Distribution of this document is unlimited.

11. SUPPLEMENTARY NOTES

12. SPONSORING MILITARY ACTIVITY

Naval Ship Systems Command
Department of the Navy
Washington, D. C. 20360

Air Force Cambridge Research Center
Lawrence G. Hanscom Field
Bedford, Massachusetts 01731

13. ABSTRACT

This report, Part II, presents additional atmospheric optical data, comparable to the data presented in Part I, but for a different type of day, and for four descents instead of two. Three of the descents were before local apparent noon; the fourth descent was after local apparent noon. Simultaneous spectral irradiance data were recorded at the surface of Crater Lake. Data presented are altitude profiles of heading of aircraft, temperature, relative humidity, equilibrium luminance, horizontal path function, attenuation length, nadir luminance, upwelling and downwelling illuminances and their ratios, reflectance calculated from nadir luminance, atmospheric beam transmittances for vertical path of sight as a function of solar zenith angle, and downwelling illuminance as a function of solar zenith angle.

DD FORM 1 JAN 64 1473

UNCLASSIFIED

Security Classification

14 KEY WORDS	LINK A		LINK B		LINK C	
	ROLE	WT	ROLE	WT	ROLE	WT
Atmospheric Optics						
Illuminance						
Transmittance						